

## Exchange anisotropy and the antiferromagnetic surface order parameter

D. Lederman,\* J. Nogués,<sup>†</sup> and Ivan K. Schuller

*Physics Department 0319, University of California—San Diego, La Jolla, California 92093-0319*

(Received 1 May 1997)

The temperature dependence of the exchange bias ( $H_E$ ) near the  $\text{FeF}_2$  Néel temperature ( $\sim 78.4$  K) was correlated with structural measurements in  $\text{FeF}_2$ -Fe bilayers. Low-angle x-ray diffraction and atomic force microscopy show that samples with larger height fluctuations have larger lateral grain sizes. Samples with larger lateral grain sizes exhibit a surface critical exponent ( $\beta_S \sim 0.8$ ) while samples with smaller grains and smaller height fluctuations have a decreased  $\beta_S$ , indicating a more three-dimensional-like phase transition or an increase in the  $\text{FeF}_2$  surface exchange interaction. [S0163-1829(97)05230-2]

The critical exponents corresponding to a bulk magnetic material and those corresponding to its surface and the atomic planes close to the surface are in general different from each other. This occurs because spins at the surface have fewer nearest neighbors than those in the bulk.<sup>1,2</sup> Early mean-field calculations<sup>3</sup> of the surface magnetization in Heisenberg ferromagnets (FM) and antiferromagnets (AF) showed that the surface order parameter has the temperature dependence  $\langle M_S \rangle \sim t^{\beta_S}$ , where  $\langle M_S \rangle$  is the surface magnetization for a FM or sublattice magnetization for an AF,  $\beta_S$  is the surface magnetization critical exponent, and  $t = 1 - T/T_C$  is the reduced temperature, with  $T_C$  representing the Curie temperature for a FM or the Néel temperature for an AF. Within the mean-field theory,  $\beta_S = 1$  and  $\beta = 0.5$ . The mean-field calculations were inspired by low-energy electron diffraction data,<sup>4</sup> which showed half-order spots induced by the appearance of antiferromagnetic order at the surface of NiO (100). Subsequent experiments<sup>5</sup> showed that  $\beta_S = 0.89 \pm 0.01$  in NiO (100). Similar behavior was later observed in ferromagnetic Ni surfaces using spin-polarized low-energy electron scattering (SPLEED),<sup>6</sup> with  $\beta_S = 0.83 \pm 0.03$ . Although the latter two values of  $\beta_S$  do not agree with the mean-field result, they do agree with more sophisticated calculations using renormalization group theory,<sup>7</sup> where  $\beta_S$  ranges from 0.78 for the 3D Ising model to 0.88 for the 3D Heisenberg model. Monte Carlo simulations not only confirmed these results,<sup>8</sup> but also demonstrated that within the Ising model  $\beta_S = 0.78$  only if the surface exchange interaction  $J_S$  is equal or smaller than the bulk  $J$ . If  $J_S > J$ ,  $\beta_S$  decreases steadily, and for  $J_S/J > 1.6$ , the surface orders at a temperature higher than the bulk  $T_C$ . This occurs because, as  $J_S$  increases, the surface tends to behave as a two-dimensional magnetic material near the phase transition, rather than the surface of a three-dimensional material. Previous mean-field calculations qualitatively agree with this result.<sup>3,9</sup> Therefore, there are three phase transition effects associated with the surface of a magnetic material: (1) the atomic layers at or near the surface order with different critical exponents than the bulk, (2) the surface critical exponent  $\beta_S$  corresponding to the order parameter of the surface is greater than the bulk exponent  $\beta$  if  $J_S/J < 1.0$ , and (3)  $\beta_S$  decreases and the surface transition temperature increases for  $J_S/J > 1.6$ .

An interesting interfacial effect occurs when an antiferro-

magnet, such as  $\text{FeF}_2$ , is placed in close proximity to a ferromagnetic material. When a ferromagnetic Fe thin film is grown on  $\text{FeF}_2$ , and the sample is field cooled through the  $\text{FeF}_2$  Néel temperature, an exchange anisotropy arises.<sup>10</sup> This exchange anisotropy is characterized by a shift of the  $M-H$  loop away from  $H=0$ , commonly denoted as the exchange bias  $H_E$ . Although this effect was discovered many years ago,<sup>11</sup> the detailed mechanism remains unclear. In the simplest model, the exchange bias arises from interface magnetic exchange, and is given by  $H_E = 2J_I S_A S_F / M_F t_F a^2$ , where  $J_I$  is the interface exchange energy,  $S_A$  and  $S_F$  are the spins of the antiferromagnet and ferromagnet,  $M_F$  is the magnetization of the ferromagnet,  $t_F$  the thickness of the ferromagnet, and  $a$  is the interface lattice parameter.<sup>11</sup> This model is inadequate for two reasons: (1) the values it yields for  $H_E$  are usually one to two orders of magnitude larger than determined from experiment, assuming that  $J_I$  has the same magnitude as the exchange interaction in the bulk FM, and (2) interface disorder or magnetically compensated surfaces would destroy  $H_E$ , while in practice the effect is observed in both cases.<sup>10,12</sup> More sophisticated models rely on domain wall creation, either parallel to the interface, created during the cool-down procedure,<sup>13</sup> or the rotation of the FM magnetization,<sup>14</sup> respectively. An important common feature of these models is that  $H_E$  is proportional to the strength of the interface magnetic interaction if the AF has uniaxial magnetic anisotropy. Moreover, because the AF domain wall size is independent of temperature for AF with uniaxial anisotropies, the model based on domain creation during cooling is only proportional to the interface interaction.<sup>15</sup> Hence, if the FM Curie temperature is much larger than the AF Néel temperature  $T_N$ ,  $H_E$  reflects the order parameter of the AF surface near  $T_N$  because in the temperature range of interest the FM magnetization is almost constant.

In the present study we investigate the surface order parameter of antiferromagnetic  $\text{FeF}_2$  by measuring the exchange bias of  $\text{FeF}_2$ -Fe bilayers near the  $\text{FeF}_2$   $T_N$ . This approach is experimentally easier than the SPLEED technique, but is limited to films that exhibit exchange bias and have an AF with strong uniaxial anisotropy. We find that  $H_E \sim t^{0.80 \pm 0.04}$  for samples with large grain sizes, with the exponent decreasing as the grain size becomes smaller. For the large grain size samples, the exponent agrees with predictions of surface ordering of the three-dimensional (3D)

Ising model. The decrease in exponent as the grain size decreases may be due either to an effective decrease in lateral terrace size or an increase in the interface exchange interaction with decreasing roughness.

The  $\text{Fe}^{2+}$  ions in  $\text{FeF}_2$  form a body-centered tetragonal crystal structure ( $a=b=4.69$  Å,  $c=3.301$  Å),<sup>16</sup> with the ions at the center of the unit cell ordering antiferromagnetically with the ions at the corners.<sup>17</sup>  $\text{FeF}_2$  has a large uniaxial magnetic anisotropy ( $K\sim 1.39\times 10^8$  erg/cm<sup>3</sup>) along the  $c$  axis.<sup>18</sup> Because of its large anisotropy,  $\text{FeF}_2$  behaves as an Ising model system over a wide temperature range.<sup>19</sup>

The growth of  $\text{FeF}_2$ -Fe bilayers on MgO (100) has been described elsewhere.<sup>10</sup> Briefly, the films were grown by sequential  $e$ -beam evaporation of  $\text{FeF}_2$  ( $t_A\sim 90$  nm at a rate of 0.2 nm/s) and Fe ( $t_F\sim 14$  at a rate of 0.1 nm/s) with the rates controlled by a calibrated quartz crystal oscillator. Substrates were heated to 450 °C for 900 s prior to deposition in order to reduce the brucite layer on the MgO substrates, then cooled to the  $\text{FeF}_2$  growth temperature  $200\leq T_S\leq 300$  °C. At these temperatures the  $\text{FeF}_2$  grows quasiepitaxially along the (110) direction with two in-plane domains. The Fe layers were deposited at 150 °C, resulting in polycrystalline films with mostly (110) and (100) orientations, and then capped with  $\sim 9$  nm of Ag to prevent oxidation. The pressure during deposition was  $<1\times 10^{-6}$  Torr.

Samples were cooled from 120 K through the  $\text{FeF}_2$  critical temperature [ $T_N=78.4$  K (Ref. 19)], to 10 K in the presence of a magnetic field  $H_{\text{FC}}=2$  kOe. The Fe  $M$ - $H$  loops were measured using a SQUID magnetometer in the  $-2$  kOe to  $+2$  kOe range (Fig. 1, top inset). In all cases, 2 kOe was enough to saturate the magnetization of the films. The Fe magnetization was measured every 5 Oe near  $M=0$  in order to determine  $H_E$  more accurately.

Figure 1 shows the typical behavior of  $H_E$  near the  $\text{FeF}_2$  Néel temperature for a sample with  $t_A=100$  nm  $\text{FeF}_2$  layer grown at 300 °C and  $t_F=14$  nm.  $H_E$  was determined from the  $M$ - $H$  loop (top inset). The  $H_E$  data were fit to a ‘‘rounded’’ power law:

$$H_E = \frac{H_{E0}}{\delta_T \sqrt{2\pi}} \int_0^\infty t_0^{\beta_S} \exp[-(T_C - T_{C0})^2 / 2\delta_T^2] dT_{C0}, \quad (1)$$

where  $t_0=1-T/T_{C0}$  for  $T<T_{C0}$  and  $t_0=0$  for  $T>T_{C0}$ .  $H_{E0}$  is the exchange bias at  $T=0$ ,  $T_C$  is the center of the critical temperature distribution, and  $\delta_T$  is its width. This equation is valid for a Gaussian distribution of transition temperatures, of width  $\delta_T$ , due to disorder, strain, or other defects. The parameters  $\beta_S$ ,  $T_C$ ,  $\delta_T$ , and  $H_{E0}$  were simultaneously fit. The errors from these parameters were estimated by fitting all parameters but one and plotting  $\chi^2$  vs each fixed parameter. The uncertainty for  $\beta_S$  was  $\pm 0.04$ . The solid line in Fig. 1 is a result of this fit. The bottom inset shows the data in a log-log scale, where the straight line is a power law with  $\beta_S=0.8$ .  $\delta_T$  was approximately  $0.7\pm 0.2$  K for all samples, regardless of the transition temperature. Given that the samples had different amounts of interface disorder (see below) yet similar values of  $\delta_T$ , the rounding could also be due to the Fe magnetically ordering the  $\text{FeF}_2$  at a temperature above the  $T_N$  of  $\text{FeF}_2$ .

In order to determine the effects of the interface structure, the  $\text{FeF}_2$  was grown at different temperatures in the

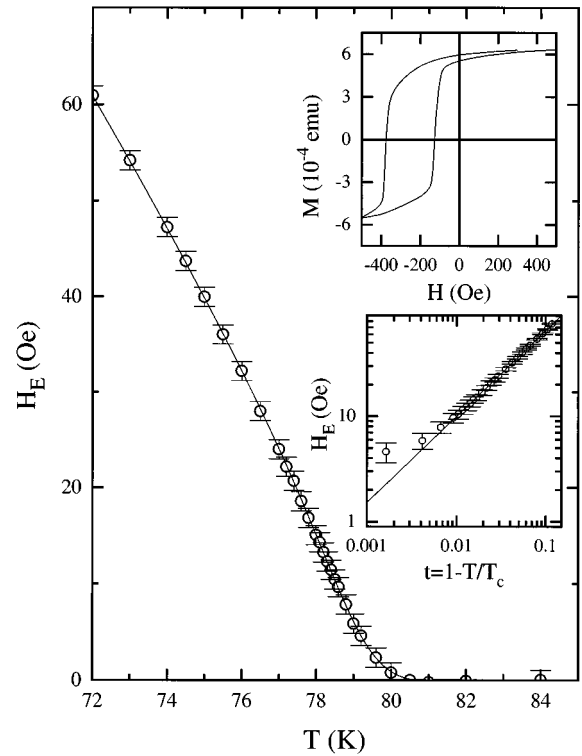


FIG. 1.  $H_E$  as a function of temperature near  $T_C$  for a sample with the 100 nm  $\text{FeF}_2$  layer grown at 300 °C and an Fe thickness  $t_F=14$  nm. The solid line is a result of a fit to Eq. (1), with  $T_C=79.33\pm 0.2$  K,  $\delta_T=0.7\pm 0.2$  K,  $\beta_S=0.80\pm 0.04$ , and  $H_{E0}=718\pm 34$  Oe. Top inset:  $M$ - $H$  loop at 10 K for the same sample after field cooling.  $H_E$  is the displacement of the center of the loop away from  $H=0$ . Bottom inset: log-log graph of  $H_E$  vs the reduced temperature  $t$ . The straight line is the power law  $H_E \propto t^{0.80}$ .

$200\leq T_S\leq 300$  °C range. Small-angle x-ray diffraction<sup>20,21</sup> and atomic force microscopy techniques were used to quantitatively analyze the interface structure. In general, samples grown at higher temperatures had larger thickness fluctuations (roughness) as well as larger lateral correlation lengths (grain size).<sup>10</sup> By fitting the x-ray data to an optical model which takes into account the diminished reflectivity at each interface due to disorder,<sup>22</sup> roughness parameters were obtained for some of the samples. It was difficult to fit, using this model, data from samples that were too rough (i.e., which did not show many low-angle peaks).

It is known that the magnitude and sign of  $H_E$  in the  $\text{FeF}_2$ -Fe system depends strongly on the cooling field,  $H_{\text{FC}}$ .<sup>23</sup> However, it is important to note that despite these changes in  $H_E$ , we found that  $\beta_S$  remains unchanged as a function of  $H_{\text{FC}}$ .

The interface magnetic energy is defined as  $\Delta E=2M_F t_F H_E$ , where  $M_F=1740$  G is the magnetization of Fe at low temperatures and  $t_F$  is the Fe thickness. In Fig. 2 we show  $\Delta E$  as a function of the parameter  $\sigma$  obtained for the Fe-Ag interface, which represents the film’s average thickness fluctuations. As has been previously discussed,<sup>10</sup>  $\sigma$  for this interface must be related to the  $\sigma$  at the  $\text{FeF}_2$ -Fe interface because, for these samples with similar  $\text{FeF}_2$  and Fe thicknesses (to within 10%), the growth temperature of the  $\text{FeF}_2$  was the only growth parameter which varied from

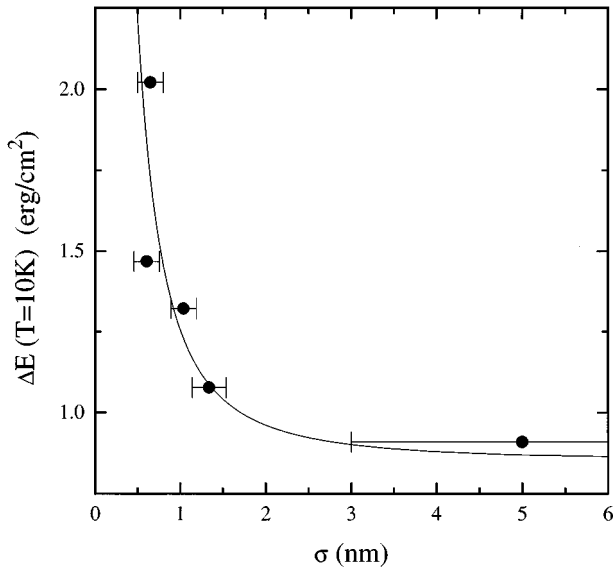


FIG. 2.  $\Delta E$  vs Fe-Ag interface roughness  $\sigma$  obtained from grazing x-ray diffraction analysis for different samples. The solid curve is a guide to the eye. Note that samples with larger  $\sigma$  also have larger terraces (island size).

sample to sample. The parameters obtained for the FeF<sub>2</sub>-Fe interface had large uncertainties, presumably due to the lower contrast between FeF<sub>2</sub> and Fe, and are thus unreliable. It is clear from these data that the exchange bias tends to decrease as  $\sigma$  increases. However, it is important to keep in mind that samples with larger values of  $\sigma$  have larger lateral grain sizes  $\xi_g$ .<sup>10</sup> As will be shown below, it is the changes in  $\xi_g$  that cause  $\beta_S$  to vary.

The critical exponent  $\beta_S$  for all samples, including those whose x-ray spectra were not fit, are shown in Fig. 3 as a function of  $\Delta E$ . The general trend is for  $\beta_S$  to decrease as  $\Delta E$  increases. Because  $\Delta E$  decreases as  $\xi_g$  (and  $\sigma$ ) increases (compare with Fig. 2),  $\beta_S$  decreases as  $\xi_g$  decreases. Note that for the samples with larger  $\xi_g$  (samples with lower

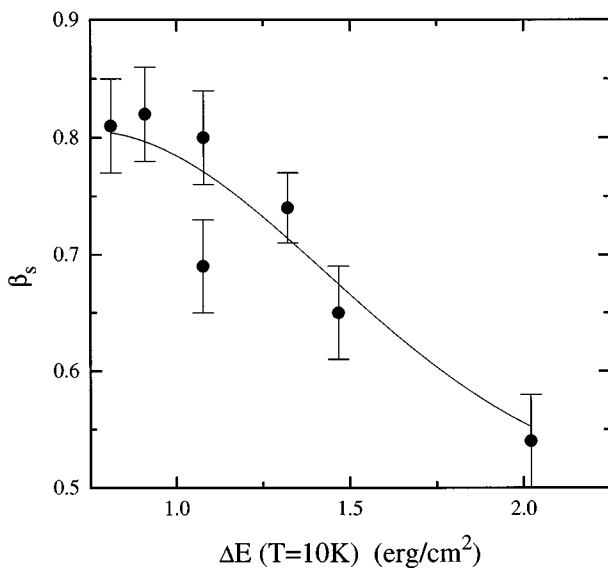


FIG. 3.  $\beta_S$  vs  $\Delta E$  for different samples. The solid curve is a guide to the eye.

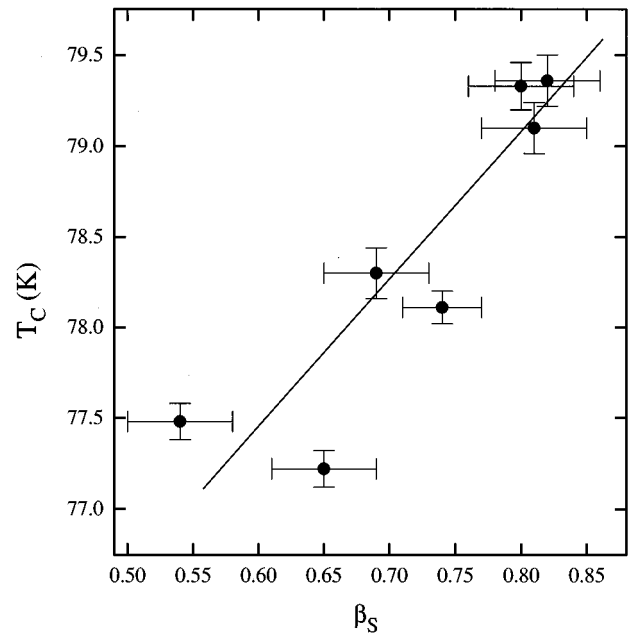


FIG. 4.  $T_C$  vs  $\beta_S$  for different samples. The straight line is a guide to the eye.

$\Delta E$ ),  $\beta_S \sim 0.80 \pm 0.04$ , which agrees well with the critical exponent of the surface of a 3D Ising system ( $\beta_S = 0.78$ ). The samples with lower values of  $\xi_g$  have a lower critical exponent, but are still significantly larger than bulk FeF<sub>2</sub> ( $\beta = 0.325$ ). This means that as  $\xi_g$  increases, the transition becomes more sensitive to the interface, i.e.,  $\beta_S$  approaches the value of the surface of a 3D Ising system. One possible reason for this behavior is related to the exchange at the FeF<sub>2</sub> surface. If the exchange at the interface is greater than in the bulk FeF<sub>2</sub>,  $\beta_S$  should be lower than 0.80 because the surface would order independently from the bulk (i.e., 2D like), tending to order with an exponent closer to the well-known 2D Ising value<sup>24</sup> of 0.125. In the range  $1.0 < J_S/J < 1.6$ , Monte Carlo simulations predict that  $\beta_S$  should decrease *without* increasing  $T_C$ , while  $T_C$  should increase for  $J_S/J > 1.6$ . Figure 4 shows  $T_C$  vs  $\beta_S$ . The changes in  $T_C$  are small, and in any case the trend is contrary to the theoretical prediction because  $\beta_S$  decreases as  $T_C$  decreases. Nevertheless, this slight decrease could be due to finite size effects, resulting from an effective reduction of the lateral correlation length of the order parameter as the terrace size decreases, which in FeF<sub>2</sub> is known to be important for sizes less than  $\sim 70$  Å.<sup>25</sup> Hence, this may indicate that  $1.0 < J_S/J < 1.6$  for all the samples. Note that  $T_C$  for some samples in Fig. 4 is larger than  $T_N = 78.4$  K, the bulk FeF<sub>2</sub> Néel temperature. This could be due to the interaction with the Fe, which would tend to order the FeF<sub>2</sub> surface at  $T > T_N$ .

Another explanation is directly related to the terrace sizes. The interface structural analysis mentioned above showed that as  $\sigma$  increases, the lateral grain size  $\xi_g$  also increases. Samples with smaller grain sizes tend to have a larger number of atoms at island or step edges which will have more nearest neighbors than atoms on the flat regions of the surface. This effectively results in a smaller value of  $\beta_S$ . However, samples with larger grains may have larger flat regions,

resulting in a value of  $\beta_S$  closer to the value corresponding to a surface  $\beta_S \sim 0.8$ . The effective value for  $\beta_S$  is a result of the average value over the whole sample, which includes averaging over regions where the Fe is in contact with FeF<sub>2</sub> atoms belonging to the second and perhaps third monolayer, as well as with atoms near corners. Hence, the exchange bias probes a distribution of values of  $\beta_S$  because of the interface disorder.

Finally, in antiferromagnets with cubic anisotropy, such as CoO or NiO, the temperature dependence of  $H_E$  is more complex. In the model proposed by Malozemoff,<sup>15</sup> for example, the temperature dependence is proportional to both the square of the order parameter in the AF bulk and to the interface order parameter for AF's with cubic anisotropy. In the present context FeF<sub>2</sub> has an intrinsic advantage, since it has a uniaxial anisotropy, and theoretically the temperature

dependence of  $H_E$  should be directly proportional only to its surface order parameter.

In conclusion, we have systematically studied the temperature dependence of the exchange bias in FeF<sub>2</sub>-Fe AF-FM bilayers as a function of interface disorder. This provides an indirect measurement of the FeF<sub>2</sub> surface order parameter. The critical exponent of  $H_E$  near  $T_C$ ,  $\beta_S$ , is found to increase as the AF film thickness fluctuations and the lateral grain size increase. This could be the result of an increase in the surfacelike exchange interaction at the interface or the presence of larger terraces as the lateral island size increases.

This work was supported by the U.S. Department of Energy under Grant No. DE-FG03-87ER45332. J.N. thanks the Spanish Ministerio de Educación y Ciencia for its financial support.

\*Present address: Physics Department, West Virginia University, Morgantown, WV 26506-6315.

<sup>†</sup>On leave from the Grup d'Electromagnetisme, Universitat Autònoma de Barcelona, Spain.

<sup>1</sup>H. Ibach and H. Lüth, *Solid State Physics* (Springer-Verlag, Berlin, 1993), p. 156.

<sup>2</sup>A. Zangwill, *Physics at Surfaces* (Cambridge University Press, Cambridge, England, 1988), p. 130.

<sup>3</sup>D. L. Mills, *Phys. Rev. B* **3**, 3887 (1971).

<sup>4</sup>P. W. Palmberg, R. E. DeWames, and L. A. Vredevoe, *Phys. Rev. Lett.* **21**, 682 (1968).

<sup>5</sup>K. Namikawa, *J. Phys. Soc. Jpn.* **44**, 165 (1978).

<sup>6</sup>S. Alvarado, M. Campagna, and H. Hopster, *Phys. Rev. Lett.* **48**, 51 (1981).

<sup>7</sup>A. J. Guttman, G. M. Torrie, and S. G. Whittington, *J. Magn. Magn. Mater.* **15-18**, 1091 (1980); H. W. Diehl and S. Dietrich, *Z. Phys. B* **42**, 65 (1981).

<sup>8</sup>K. Binder and D. P. Landau, *Phys. Rev. Lett.* **52**, 318 (1984).

<sup>9</sup>K. Binder and P. C. Hohenberg, *Phys. Rev. B* **9**, 2194 (1974).

<sup>10</sup>J. Nogués, D. Lederman, T. J. Moran, Ivan K. Schuller, and K. V. Rao, *Appl. Phys. Lett.* **68**, 3186 (1996).

<sup>11</sup>W. H. Meiklejohn and C. P. Bean, *Phys. Rev.* **102**, 1413 (1957); W. H. Meiklejohn and C. P. Bean, *ibid.* **105**, 904 (1957).

<sup>12</sup>P. J. van der Zaag, R. M. Wolf, A. R. Ball, C. Bordel, L. F. Feiner, and R. Jungbult, *J. Magn. Magn. Mater.* **148**, 346 (1995);

P. J. van der Zaag, A. R. Ball, L. F. Feiner, R. M. Wolf, and P. A. A. van der Heijden, *J. Appl. Phys.* **79**, 5103 (1996).

<sup>13</sup>A. P. Malozemoff, *Phys. Rev. B* **35**, 3679 (1987); **37**, 7673 (1988).

<sup>14</sup>D. Mauri, H. C. Siegmann, P. S. Bagus, and E. Kay, *J. Appl. Phys.* **62**, 3047 (1987).

<sup>15</sup>A. P. Malozemoff, *J. Appl. Phys.* **63**, 3874 (1988).

<sup>16</sup>J. W. Stout and S. A. Reed, *J. Am. Chem. Soc.* **76**, 5279 (1954).

<sup>17</sup>R. A. Erickson, *Phys. Rev.* **90**, 779 (1953).

<sup>18</sup>M. T. Hutchings, B. D. Rainford, and H. J. Guggenheim, *J. Phys. C* **3**, 307 (1970).

<sup>19</sup>D. P. Belanger, P. Nordblad, A. R. King, and V. Jaccarino, *J. Magn. Magn. Mater.* **31-34**, 1095 (1983).

<sup>20</sup>I. K. Schuller, *Phys. Rev. Lett.* **44**, 1597 (1980); W. Sevenhans, M. Gijs, Y. Bruynseraede, H. Homma, and I. K. Schuller, *Phys. Rev. B* **34**, 5955 (1986); E. E. Fullerton, I. K. Schuller, H. Vanderstraeten, and Y. Bruynseraede, *ibid.* **45**, 9292 (1992).

<sup>21</sup>S. K. Sinha, E. B. Sirota, S. Garoff, and H. B. Stanley, *Phys. Rev. B* **38**, 2297 (1988).

<sup>22</sup>B. Vidal and P. Vincent, *Appl. Opt.* **23**, 1794 (1984).

<sup>23</sup>J. Nogués, D. Lederman, T. J. Moran, and Ivan K. Schuller, *Phys. Rev. Lett.* **76**, 4624 (1996).

<sup>24</sup>L. Onsager, *Phys. Rev.* **65**, 117 (1944).

<sup>25</sup>D. Lederman, C. A. Ramos, V. Jaccarino, and J. L. Cardy, *Phys. Rev. B* **48**, 8365 (1993).